Science of the Total Environment 542 (2016) 757–770

Contents lists available at ScienceDirect

Science of the Total Environment

journal homepage: www.elsevier.com/locate/scitotenv

Predicting the long-term durability of hemp–lime renders in inland and coastal areas using Mediterranean, Tropical and Semi-arid climatic simulations

Anna Arizzi [a,*], Heather Viles [a], Inés Martín-Sanchez [b], Giuseppe Cultrone [c]

[a] School of Geography and the Environment, University of Oxford, Dyson Perrins Building, South Parks Road, Oxford OX1 3QY, UK
[b] Departamento de Microbiología, Universidad de Granada, Avda. Fuentenueva s/n, 18002 Granada, Spain
[c] Departamento de Mineralogía y Petrología, Universidad de Granada, Avda. Fuentenueva s/n, 18002 Granada, Spain

HIGHLIGHTS

- Realistic simulations in the cabinet of one-year exposure to environmental conditions
- Influence of the lime type on the durability of hemp–lime renders
- Improvement of the carbonation of lime under Mediterranean and Tropical conditions
- More intense colonisation of alkaliphiles fungi and bacteria under heavy rainfall
- Superficial deposition and leaching of NaCl, with no damage observed in the samples

GRAPHICAL ABSTRACT

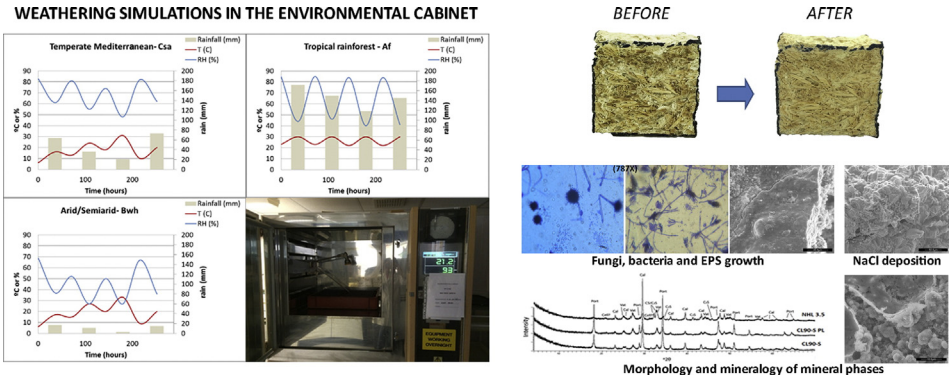

ARTICLE INFO

Article history:
Received 28 August 2015
Received in revised form 27 October 2015
Accepted 27 October 2015
Available online xxxx

Editor: D. Barcelo

Keywords:
Environmental cabinet
Rainfall
Sodium chloride
Hemp
Bio-receptivity
Bacterially-precipitated carbonates

ABSTRACT

Hemp-based composites are eco-friendly building materials as they improve energy efficiency in buildings and entail low waste production and pollutant emissions during their manufacturing process. Nevertheless, the organic nature of hemp enhances the bio-receptivity of the material, with likely negative consequences for its long-term performance in the building. The main purpose of this study was to study the response at macro- and micro-scale of hemp–lime renders subjected to weathering simulations in an environmental cabinet (one year was condensed in twelve days), so as to predict their long-term durability in coastal and inland areas with Mediterranean, Tropical and Semi-arid climates, also in relation with the lime type used. The simulated climatic conditions caused almost unnoticeable mass, volume and colour changes in hemp–lime renders. No efflorescence or physical breakdown was detected in samples subjected to NaCl, because the salt mainly precipitates on the surface of samples and is washed away by the rain. Although there was no visible microbial colonisation, alkaliphilic fungi (mainly *Penicillium* and *Aspergillus*) and bacteria (mainly *Bacillus* and *Micrococcus*) were isolated in all samples. Microbial growth and diversification were higher under Tropical climate, due to heavier rainfall. The influence of the bacterial activity on the hardening of samples has also been discussed here and related with the formation and stabilisation of vaterite in hemp–lime mixes. This study has

* Corresponding author.
E-mail address: anna.arizzi@ouce.ox.ac.uk (A. Arizzi).

http://dx.doi.org/10.1016/j.scitotenv.2015.10.141
0048-9697/

demonstrated that hemp–lime renders show good durability towards a wide range of environmental conditions and factors. However, it might be useful to take some specific preventive and maintenance measures to reduce the bio-receptivity of this material, thus ensuring a longer durability on site.

1. Introduction

Within the last two decades, growing awareness of the need to reduce the carbon footprint of buildings (i.e. reduction of gas emissions and waste and use of renewable resources) and to increase their energy efficiency has promoted the development of novel building materials that provide a sustainable and technically valid alternative to cement and synthetic polymer-based materials. Most of these novel materials are composed of an inorganic binder (e.g. lime, clay, gypsum) and plant aggregates. Flax, wool, bamboo, kenaf and, in particular, hemp are some examples of the non-food crops lately being revaluated by the construction sector (RILEM PRO99, 2015). The reason for the increasing interest in using hemp in building materials is twofold: first, its growth represents a benefit for the environment (annual crop; carbon-sequestering plant; there is no need for pesticides and fertilisers; cleaning and improvement of the soil) and second, its use in buildings favours healthier in-door spaces (buffering activity against humidity variations) and improved energy efficiency (thermal and acoustic insulation) (Pervaiz and Sain, 2003; Esmail, 2010; Tran Le et al., 2010; Faruk et al., 2012).

However, recent studies on hemp concrete and hemp–lime have shown that prolonged water absorption under moist conditions, scarce ventilation and the wrong choice of the protective coating may lead to intense bio-decay (Arizzi et al., 2015a; Bessette et al., 2015; Lamoulie et al., 2015; Marceau et al., 2015; Simons et al., 2015). The protective action of lime (which normally acts as a disinfectant), indeed, seems to be limited against alkaliphilic bacteria and fungi (Walker et al., 2014; Arizzi et al., 2015a). Although none of the isolated microorganisms induce mycosis in healthy individuals, this finding is still worrying in terms of aesthetic appearance and, more importantly, long-term performance of the hemp–lime composite in the masonry system (unless microbial colonisation is desired, such as in green buildings, Manso et al., 2014). Obviously, the exposure conditions applied in the laboratory are not the same as the climatic conditions on site, and so it would be wrong assuming that the same bio-decay would occur in the hemp–lime mixes once in the building. However, since the growth of microorganisms is strongly influenced by conditions of temperature and relative humidity (Camuffo, 2014), it is necessary to study the behaviour of hemp–lime composites under specific climatic conditions to be able to make realistic predictions on their long-term durability. To the best of our knowledge, there are few studies on the durability of hemp-based building materials in the literature. In particular, most of this research only describes the response of hemp concrete to accelerated ageing tests (common standard laboratory tests), such as wetting-drying, freezing-thawing and salt crystallisation cycles (Walker et al., 2014; Marceau et al., 2015), without studying the durability of hemp concrete under several climatic factors acting simultaneously. Furthermore, when hemp–lime composites are used as external surface protective finish (i.e. render) their susceptibility to weathering is expected to be even higher than that of hemp-based mixes used as infill. Bevan and Woolley (2008), in fact, commented that there is no firm evidence of how well the render or plaster performs when it is made with hemp–lime.

With the purpose of filling this knowledge gap, we have developed and applied new weathering tests specifically conceived to study the durability of hemp–lime renders. To obtain a more realistic response from the material, we have reproduced the environmental conditions of three selected climates typical of the geographic areas where hemp is mostly grown and/or applied in sustainable construction. The updated Köppen–Geiger's climate classification (Kottec et al., 2006) has been used to select and name the three climates listed below:

1) Warm temperate (named *Mediterranean climate*, *Csa*): characterised by warm annual temperatures, with hot and dry summer, typical of Mediterranean countries.
2) Equatorial rainforest, fully humid (named *Tropical climate*, *Af*): characterised by high annual temperature and heavy rainfall, typical of equatorial countries.
3) Arid desert (named *Semi-arid climate*, *Bwh*): characterised by large annual temperature range, dry winter, typical of hot arid countries.

For each climate, specific cycles were designed and then simulated in an environmental cabinet. The conditions in both coastal and inland areas were also simulated for each climate, taking into account the presence and absence of airborne salt (NaCl), respectively. The macroscopic characteristics of the samples (mass, volume and chromatic variations) were monitored before, during and after the weathering tests whilst chemical-mineralogical and microstructural modifications were investigated at the end of each test. Finally, microbiological tests were performed to study how the bio-receptivity of hemp–lime composites is influenced by the climatic conditions (especially RH variations, Jain et al., 2009; Johansson et al., 2014, and rainfall, Caneva et al., 1992) and the presence of sodium chloride (e.g. growth of different number or type of microbe species), taking into account that soluble salts may affect microorganism growth, favouring halophilic (i.e. salt tolerant) species (Altieri and Pinna, 2005). The influence of the type of lime (aerial dry hydrated and putty and natural hydraulic) on the durability of the hemp–lime mixes has also been studied in this work.

2. Materials and methods

2.1. Hemp–lime samples

Three types of hemp–lime mixes were prepared in the same way as in a previous study (Arizzi et al., 2015a), to compare the response of the materials under laboratory and simulated realistic conditions. Hemp shiv (Cannhabitat®, produced by AgroFibre, Euralis, Cazeres, France, and supplied by Cannabric, Guadix, Granada, Spain) were mixed with dry hydrated lime (CL90S, BS-EN 459-1, 2010, produced by ANCASA, Seville, Spain), lime putty (CL90-S PL, BS-EN 459-1, 2010, produced by ComCal, Barcelona, Spain), and natural hydraulic lime (NHL3.5, BS-EN 459-1, 2010, produced by Socli, Italcementi Group, Izaourt, France) in a lime:hemp:water dosage by volume of 3:5:2.5. Mixes were named as C, N and P, according to the type of lime (CL90S, NHL 3.5 and CL90S PL, respectively), and they were cured under T = 17 °C and RH = 75% for three months before the study. For more information on the binder choice and the mix procedure, dosages and conditions refer to Arizzi et al. (2015a).

In total, 36 hemp–lime mix samples were tested, giving four samples per composite type under each climatic simulation (half of them were subjected to salt attack). In the cabinet, samples ($2 \times 4 \times 4$ cm^3) were placed with the largest surface (4×4 cm^2) facing the water hose, so as to reproduce the exposure conditions of a render (with the largest surface facing the external conditions).

2.2. Simulations of the climatic conditions in the environmental cabinet

Climatic simulations were carried out in a Sanyo-FE 300H/MP/R20 environmental cabinet (inner volume: $675 \times 630 \times 650$ mm^3). Four

different cities or countries within the same climate zones (Rome, Athens, Seville and Los Angeles for the Mediterranean climate; Suriname, Samoa, Congo and Indonesia for the Tropical climate; Nevada, Western Sahara, Iraq and Granada for the Semi-arid climate; see Supplementary material SM 1) have been taken as a reference to establish the average values of the conditions of temperature (T) relative humidity (RH) and rainfall (recorded in 2012) to be reproduced in the cabinet for each climate (Fig. 1).

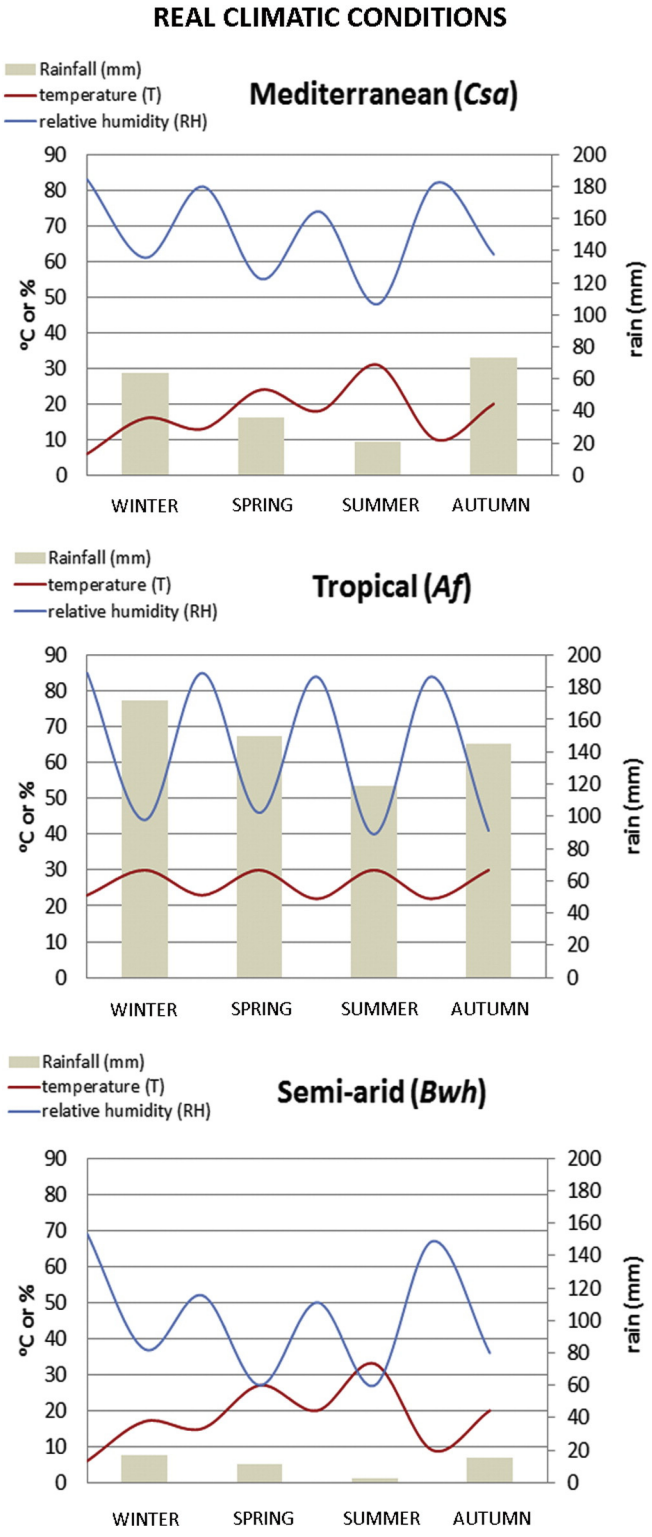

Fig. 1. Average conditions of temperature (T, in °C), relative humidity (RH, in %) and rainfall (in mm) recorded for a whole year (2012) in four different cities or countries within the same climate zones (Mediterranean, Tropical and Semi-arid).

For each climate, the whole year has been simulated by downscaling the monthly conditions in the cabinet, with one year of real climatic conditions condensed into 12 days in the cabinet (288 h). To allow time for the samples to adapt to these conditions, especially for the microbes to adapt to the monthly conditions, these were simulated over 8 h and repeated three times every day (each month lasted 24 h in the cabinet). The first month simulated was March, as renders are usually applied in spring. The three climatic conditions were tested in the cabinet prior to the weathering test and were recorded every 120 min by means of data loggers (iButton™). The main differences between the programmed conditions (i.e. expected conditions) and those reproduced by the cabinet during the tests (i.e. test conditions) can be found in the RH values that are harder to accurately reproduce in the cabinet, compared to the T values (Fig. 2).

2.2.1. Rainfall simulations

Rainfall (mist or heavy rain) was simulated by means of a hose placed inside the cabinet. The amount of water sprayed during each test, detailed in Table 1, was calculated by converting mm of rain into mL of water, using an experimental rain gauge. The volume value was then converted into spraying period (in min), after recording the quantity of water (in mL) dispensed by the hose at constant flow rate (in the "mist" spraying mode, the hose dispenses 10 mL of water in 60 s whilst, in the "cone" mode, the hose dispenses 10 mL in 15 s). Only the most intense rainy periods were simulated in the cabinet, and the nature of the spraying events (indicated by green arrows in Fig. 2) was adjusted according to the climatic conditions (SM 1). In the Mediterranean and Semi-arid tests, water was only sprayed between autumn and winter (Fig. 2) using mist mode and its amount corresponded to the sum of the average precipitation recorded within a whole year (TOT value in Table 1). In the Tropical test, instead, the periodic rainfall typical of this climate was simulated using cone mode at the beginning of every simulated season (Fig. 2), and the amount corresponded to the average seasonal precipitation (Table 1).

After spraying, water was collected in a tray and quickly removed from the cabinet to avoid humidity changes or freezing phenomena.

2.2.2. Salt exposure

To study the effect of airborne salt in coastal areas, half samples were also subjected to salt attack during the climatic simulations. Preliminary weathering tests showed that when the salt solution is applied by spraying samples during the test, most of the salt is washed away after the rainfall period in the cabinet (Arizzi et al., 2014). Therefore, samples were priory soaked in a half-saturated NaCl solution (18 g NaCl/100 mL water) for 90 min and then oven-dried for 5 h. These samples, like those without salt, were then subjected to rainfall simulations during the experiment in the cabinet.

2.3. Limitations of the research approach

Simulating climatic conditions in an environmental cabinet make the weathering tests much more realistic than the standardised ones. However, this experimental approach still presents some limitations, as commented below in relation with this study:

a) *Length of the test*: One weathering cycle, corresponding to one year condensed in twelve days, is obviously not sufficient to fully predict the durability that the renders will exhibit in the building, where they will be exposed to the same conditions repeatedly and for a longer period of time.
b) *Size of samples*: small samples will respond differently than in a real render, due to a number of factors, such as: larger surface area of the render; influence of the hygrothermal properties of the support; wind conditions.

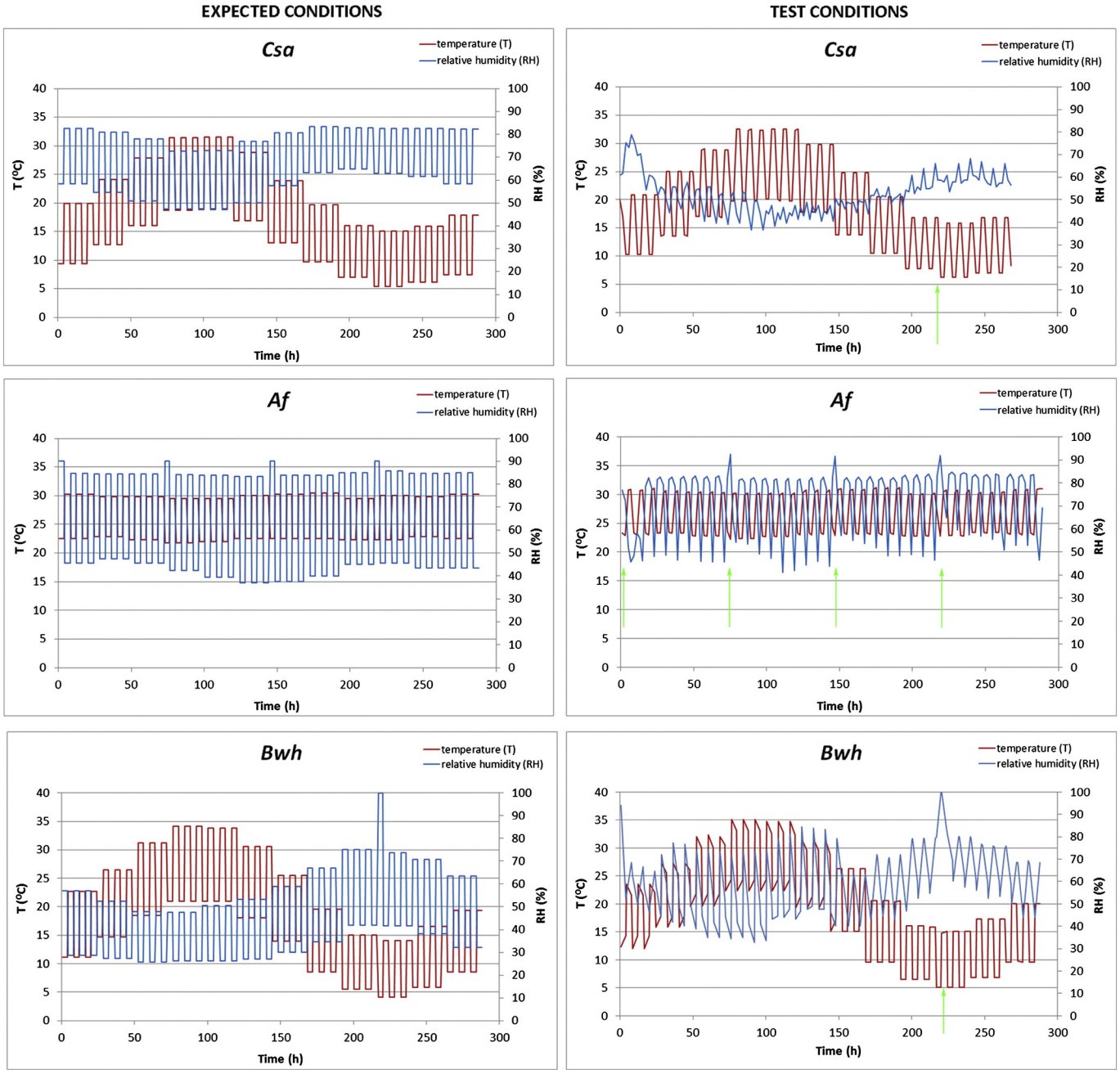

Fig. 2. Expected and test conditions of temperature (T, in °C) and relative humidity (RH, in %) for the Mediterranean (*Csa*), Tropical (*Af*) and Semi-arid (*Bwh*) climates. Green arrows indicate the rainfall events. (For interpretation of the references to colour in this figure legend, the reader is referred to the web version of this article.)

c) *Microbial communities*: the microorganisms growth is potentially more intense in-situ (more species are expected to be isolated), but our experiments can still demonstrate what grows and what does not grow depending on the environmental conditions.
d) *Salt attack simulation*: sodium chloride is obviously not the only salt that can potentially deteriorate hemp–lime renders, if we consider other sources of salts apart from the sea (e.g. soil; adjacent building materials; etc.).

Despite the limitations described above, the present work still represents an important step in the comparative study that needs to be undertaken before the use of any building and repair materials. Moreover, comparing the weathering behaviour of hemp mortars made with different lime types is helpful to decide which type of lime is most suitable under specific environmental conditions.

2.4. Macroscopic investigations during the weathering tests

Samples were weighed (to an accuracy of ±0.01 g), and photos taken at the end of each day of the test (i.e. a simulated month), in order to record any visible change in samples.

The following chromatic parameters of hemp–lime samples were determined by means of a portable Konica-Minolta CM-700d spectrophotometer: L^* (lightness), a^* and b^* (colour coordinates) according to the CIELab colour space system (BS-EN 15886, 2010); Y (yellow, calculated according to ASTM E313-15 2015) and W (whiteness, calculated according to the Stansby method) indices. The measurement

Table 1
Average seasonal precipitation (in mm converted to mL) recorded during 2012 in four different cities and countries with Mediterranean (*Csa*), Tropical (*Af*) and Semi-arid (*Bwh*) climates, and converted into rainfall duration (in min) in the cabinet, according to the spraying mode of the hose (mist and cone). In bold the spraying duration (in min) finally simulated in each weathering test.

Csa			
	mm	mL	min (mist mode)
Winter	85	64	6
Spring	48	36	4
Summer	28	21	2
Autumn	97	73	7
TOT	258	194	**20**
Af			
	mm	mL	min (cone mode)
Winter	228	172	**4**
Spring	198	150	**4**
Summer	158	119	**3**
Autumn	193	145	**4**
TOT	777	–	–
Bwh			
	mm	mL	min (mist mode)
Winter	22	17	2
Spring	14	11	1
Summer	4	3	0
Autumn	20	15	2
TOT	60	46	**5**

conditions were as follows: 380–780 nm spectral range, with acquisition data every 10 nm, measurement area of 8 mm, D65 CIE standard illuminant, 10° standard colorimetric observer and SCI/SCE modes (BS-EN 15886, 2010). Three faces were analysed: the largest face exposed to rainfall (4×4 cm^2), the largest opposite face (4×4 cm^2) and one of the side faces (2×4 cm^2). Six measurements per face were performed, giving a total of eighteen measurements per specimen. The overall colour difference (ΔE^* on the L^*, a^* and b^*values, BS-EN 15886, 2010) of the three mortar types before and after the weathering tests was also determined as follows: $\Delta E = \sqrt{((L_1^*-L_2^*)^2 + (a_1^*-a_2^*)^2 + (b_1^*-b_2^*)^2)}$, where L_1^*, a_1^* and b_1^* are respectively the lightness and the chromatic coordinates of the control samples and L_2^*, a_2^* and b_2^* are those of the weathered samples.

2.5. Microscopic investigations after the weathering tests

At the end of the weathering simulations, samples were removed from the cabinet and stored under laboratory conditions (T = 20 °C and RH = 60%) for one week before their mineralogical, microstructural and microbiological study. The same storage conditions were applied to the control samples. The mineralogy of hemp–lime mixes was studied by means of X-ray diffraction (XRD) analysis, using a Panalytical X'Pert PRO MPD diffractometer (with automatic loader). Analysis conditions were: radiation CuKα (λ = 1.5405 Å), 3 to 60 °2θ explored area, 45 kV voltage, 40 mA current intensity and goniometer speed using a Si-detector X'Celerator of 0.01 °2θ/s. The interpretation and identification of the mineral phases was performed using the X-Powder© software (Martín Ramos, 2004). The mineralogy of weathered samples was compared to that of control samples (non-weathered samples, both treated and untreated with salt) left for the same period under laboratory conditions.

Microscopic observations of the samples were performed by means of a Philips Quanta 400 environmental scanning electron microscope (ESEM coupled with a Genesis EDAX, with Si(Li) detector SUTW), which worked at a fixed temperature of 2 °C. Small pieces collected from the sample surface (~5 mm^2, including matrix and hemp shiv) were directly put in the chamber, which was initially purged 5 times at a range of pressures between 2.5 and 5.5 Torr (RH ~ 50% and 100% at T = 2 °C). Once equilibrium was achieved, pressure was fixed at 2.7 Torr (RH ~ 55% at T = 2 °C). Control samples (non-weathered, treated with salt), left for the same period under laboratory conditions, were also observed by ESEM to be compared with the samples subjected to weathering tests in the cabinet and pre-treated with salt.

A microbiological study was performed on the samples after the weathering tests and on the control samples (non-weathered, treated and untreated with salt). Swab samples (sterilised by ethylene oxide and individually wrapped in peel-pack) deemed suitable for isolations in culture media (Class IIa) (Eurotubo, Deltalab, Rubí, Spain) and adhesive tape samples were collected to characterise the microbial community present in the hemp–lime mixes. Samples were inoculated onto Petri plates containing Trypticase soy agar (TSA, Scharlau Chemie S.A., Barcelona, Spain) and Sabouraud chloramphenicol agar (Scharlau) media (100 μL of the suspension obtained per plate) and incubated at 28 °C for one week. During this period, colonies exhibiting different morphology and appearance were transferred to new culture plates of TSA medium for bacteria and potato dextrose agar (PDA) for fungi, to obtain pure strains. Phenotypic characterisation of isolated microorganisms was performed by observation of macroscopic features such as colour, shape and texture of colonies that appeared in the culture media. Hyphae, sporangia and spores of fungi have been visualised by staining with lactophenol blue. Bacteria were identified by Gramme staining. Observation of the samples was performed with a Leitz Dialux 22 optical microscope and images were obtained with an Olympus Camedia C-5060 camera coupled to the microscope.

3. Results and discussion

3.1. Macroscopic changes

3.1.1. Sample mass variations

From Fig. 3 (especially from Csa and Bwh curves), it is possible to see that temperature and relative humidity changes did not cause a significant mass variation in samples. The most significant changes were recorded instead after the rainfall events (indicated by green arrows in Fig. 3). The mass increase caused by water absorption during these events was proportional to both the spraying duration and the amount of sprayed water, being greater in samples subjected to the Tropical weathering test (Af). Interestingly, only one day after the Af rainfall events, samples lost most of the gained weight apart from an additional 0.5% of residual weight recorded before each new rainfall event. At the end of the Af weathering test, indeed, samples increased their weight by approximately 2%. This is the consequence of the hysteresis hygric behaviour of hemp composites (Aït Oumeziane et al., 2015), which is due to the fact that, even after drying, the hemp shiv remain partially swollen and this increases their capacity to absorb water (Arizzi et al., 2015a).

Samples with salt showed similar behaviour, apart from a great weight loss recorded during the first days in the cabinet and caused by the slow water evaporation after immersion under the salt solution (see Supplementary material, SM 2). At the end of the Bwh simulations, samples with salt gained more weight compared to those without salt, owing to the hygroscopic nature of NaCl salt.

Among the three hemp–lime mixes, those made with lime putty (P) seem to be more sensitive to T and RH conditions and especially to rainfall events, which caused a bigger water absorption (mass increase) in P samples not subjected to salt attack. This trend seems to be inverted when samples are pre-treated with salt (see Csa and Af test with salt in Fig. 3). Notwithstanding, in all weathering tests, P samples absorbed the largest volume of salt solution (see Supplementary material SM2) and this has caused an even greater absorption of water during the weathering tests with salt. The reason why this is not reflected in the Csa and Af mass variation curves of P samples is that the greater the

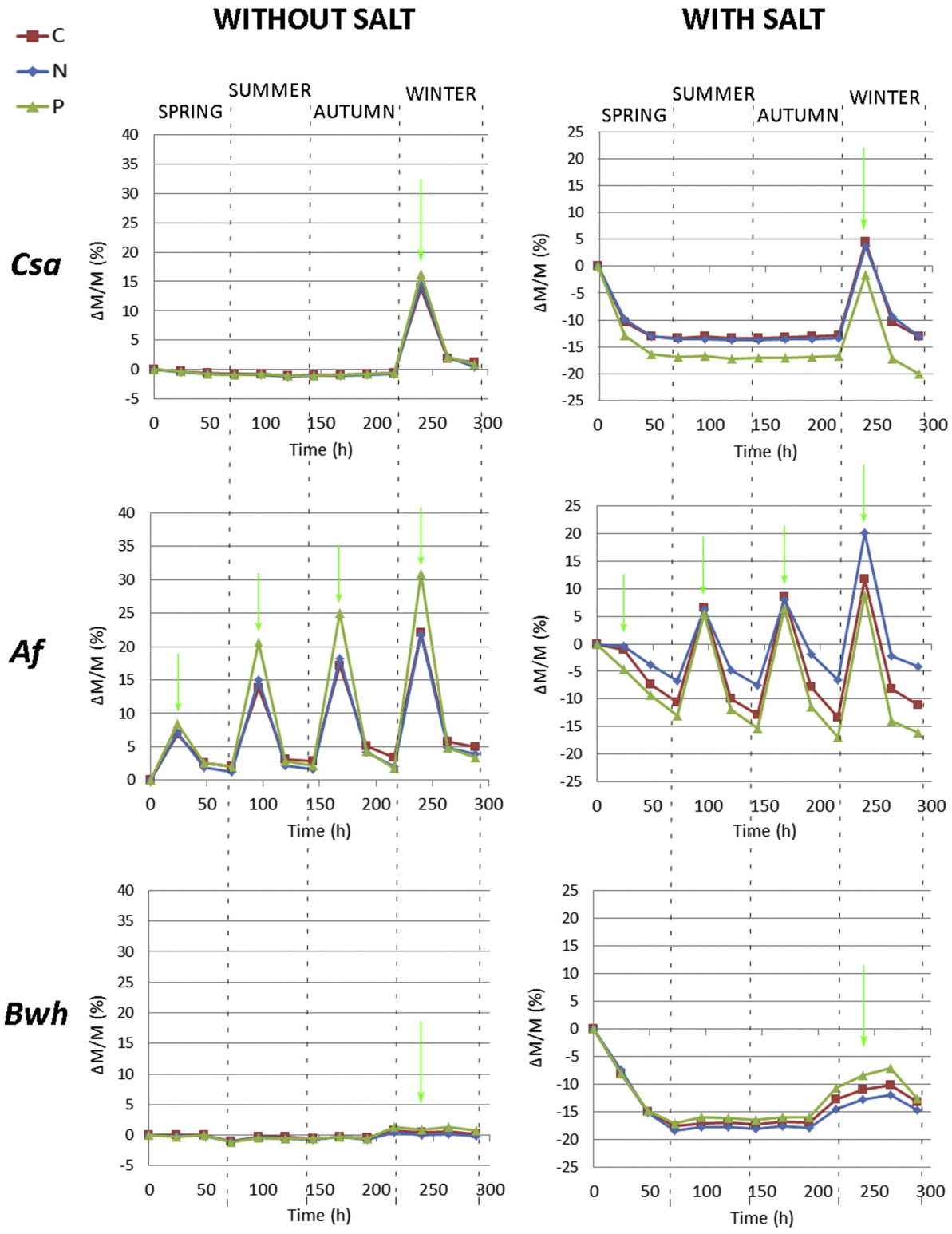

Fig. 3. Sample mass variation (ΔM/M, in %) as a function of time (in hours, h) during the Mediterranean (*Csa*), Tropical (*Af*) and Semi-arid (*Bwh*) weathering tests. Samples subjected (with salt) or not subjected (without salt) to salt attack. Legend: C, CL90S + hemp shives mix; N, NHL 3.5 + hemp shives mix; P, CL90S PL + hemp shives mix. Green arrows indicate the rainfall events. (For interpretation of the references to colour in this figure legend, the reader is referred to the web version of this article.)

amount of water absorbed during the test the greater the quantity of salt washed away from the sample, with an overall lower weight increase in P samples compared to C and N ones. The greater water and salt absorption ability of hemp-based composites made with lime putty (CL90S PL) compared to those made with dry-hydrated lime (CL90S) and natural hydraulic lime (NHL3.5) was also found in a previous study (Arizzi et al., 2015a) and it is certainly linked to the pore system of these composites.

3.1.2. Sample appearance and chromatic variations

The appearance of samples was only slightly affected by the weathering simulations in the cabinet. In samples not subjected to salt

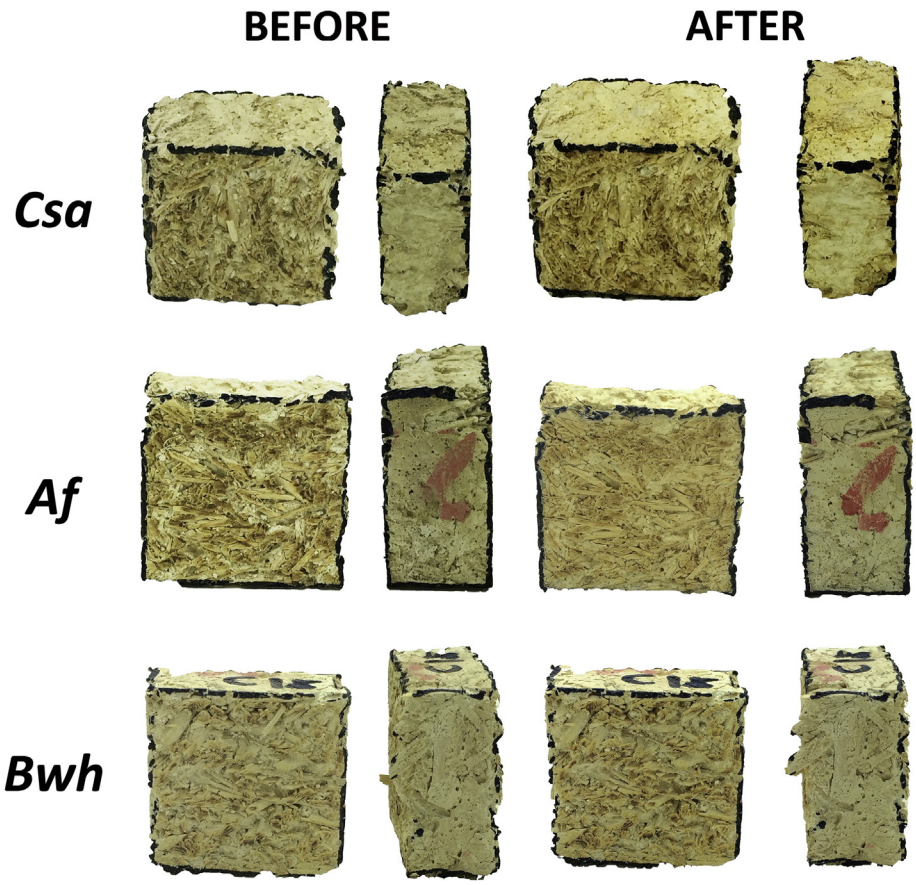

Fig. 4. Appearance of the C samples (CL90S + hemp shives mix) not-subjected to salt attack before and after the Mediterranean (*Csa*), Tropical (*Af*) and Semi-arid (*Bwh*) weathering tests.

attack, the only perceivable modification was a slight brightening of the surface, especially visible in samples subjected to Af conditions (Fig. 4). The periodic rainfall reproduced during the Af test, together with the bigger amount of water dispensed by the hose and the heavier spraying (cone mode), have induced a more intense sample cleaning (removal of dirtiness coming from the saw used to cut the samples). This effect is not so evident in the other samples subjected to Csa and Bwh conditions, therefore we can infer that RH and T changes and low rainfall do not have a visible influence on the colour of hemp–lime mixes.

Fig. 5 illustrates key trends (ΔE^*, overall colour change) for the colour data reported in Table 2. The Mediterranean climatic conditions (Csa, Fig. 5) induced the greatest colour change in samples, especially in those made with aerial lime (C, with dry hydrated lime and P, with lime putty). C samples untreated with salt, indeed, suffered the highest yellowing (Y value increased by 13, Table 2) and loss of whiteness (W value decreased by 17, Table 2), with a resulting decrease in lightness (L^* value decreased by 3, Table 2).

Different chromatic modifications were found in samples pre-treated with salt, especially those made with lime putty (P) and subjected to Csa conditions. Those samples experienced almost no changes in whiteness (W, Table 2) and an increase in lightness (L value decreased by 8, Table 2) that was responsible for their overall colour change (Fig. 5). In general, all samples pre-treated with salt became whiter because of the formation of white efflorescences on the surface of samples (especially P samples, see Fig. 6). However, the deposition of salt was only superficial and did not cause any aesthetic damage to the samples, as it was easily washed away during the rainfall period, and only a hardly visible white stain remained on the sample surface (as indicated by the red arrows in Fig. 6, after winter).

It is worth highlighting that none of the chromatic variations previously observed and measured after standard tests on the same hemp–

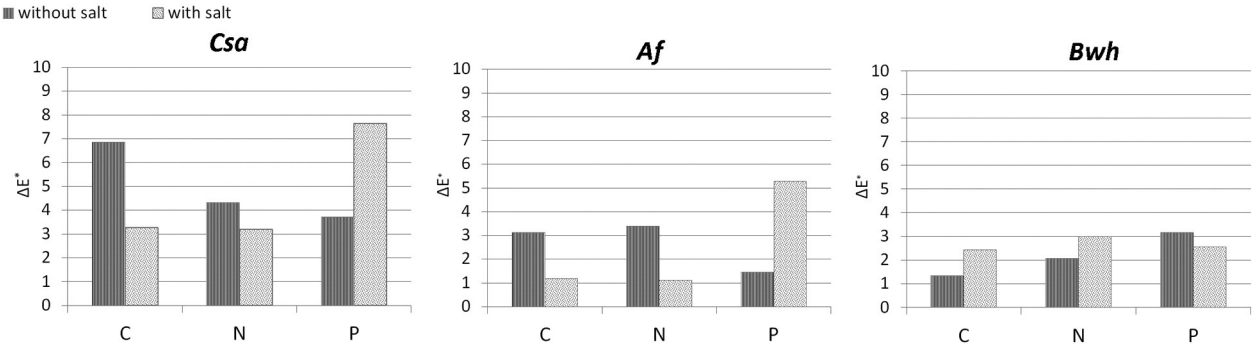

Fig. 5. Overall colour difference (ΔE^*) of hemp–lime samples during and after the Mediterranean (*Csa*) Tropical (*Af*) and Semi-arid (*Bwh*) weathering tests. Legend: C, CL90S + hemp shives mix; N, NHL 3.5 + hemp shives mix; P, CL90S PL + hemp shives mix.

Table 2
Chromatic parameters (L^*, lightness; a^* and b^*, colour coordinates; Y, yellow index; W, whiteness index) measured on samples before and after the Mediterranean (*Csa*), Tropical (*Af*) and Semi-arid (*Bwh*) weathering tests. Legend: C, CL90S + hemp shives mix; N, NHL 3.5 + hemp shives mix; P, CL90S PL + hemp shives mix.

	Without salt					With salt				
	L^*	a^*	b^*	Y	W	L^*	a^*	b^*	Y	W
Csa										
C samples										
Before	75.1 ± 5.3	3.6 ± 1.2	19.0 ± 2.0	43.2 ± 7.1	28.8 ± 7.5	76.9 ± 4.8	3.4 ± 1.1	18.9 ± 3.0	42.2 ± 8.2	30.2 ± 10.4
After	72.3 ± 7.2	4.6 ± 2.2	25.1 ± 3.3	56.6 ± 10.9	10.7 ± 10.0	78.2 ± 4.7	3.4 ± 1.1	21.9 ± 4.0	46.7 ± 9.7	22.6 ± 13.6
N samples										
Before	79.2 ± 4.4	3.1 ± 1.1	17.7 ± 2.9	38.9 ± 8.0	35.4 ± 10.1	78.5 ± 4.7	3.4 ± 1.2	19.1 ± 3.5	41.8 ± 9.1	31.5 ± 11.8
After	77.7 ± 5.6	3.2 ± 1.5	21.8 ± 3.8	46.8 ± 10.5	22.0 ± 12.6	77.2 ± 4.7	3.4 ± 1.3	22.0 ± 3.9	47.4 ± 9.7	21.6 ± 12.4
P samples										
Before	72.1 ± 1.2	5.0 ± 0.7	24.7 ± 2.4	55.8 ± 5.5	13.0 ± 6.4	70.6 ± 2.6	5.2 ± 0.5	22.8 ± 0.5	53.5 ± 1.0	17.7 ± 0.4
After	70.2 ± 2.9	6.3 ± 0.2	27.6 ± 1.7	63.0 ± 0.9	6.4 ± 3.0	78.1 ± 4.7	4.0 ± 0.7	23.8 ± 3.3	50.6 ± 8.1	18.6 ± 12.3
Af										
C samples										
Before	74.2 ± 5.0	3.8 ± 1.4	19.5 ± 3.5	44.8 ± 9.7	27.0 ± 11.4	71.2 ± 5.7	4.9 ± 0.9	20.4 ± 3.0	48.8 ± 8.9	24.8 ± 12.1
After	76.4 ± 5.3	3.6 ± 1.7	21.8 ± 4.0	47.7 ± 10.6	21.8 ± 12.3	72.2 ± 6.3	4.5 ± 1.4	20.8 ± 3.2	48.8 ± 9.5	23.1 ± 11.1
N samples										
Before	78.0 ± 3.8	3.3 ± 1.0	18.6 ± 2.8	40.9 ± 7.3	32.3 ± 9.3	77.4 ± 4.2	3.5 ± 0.8	19.0 ± 3.5	42.1 ± 8.6	30.9 ± 12.3
After	76.1 ± 4.0	3.7 ± 1.0	21.4 ± 2.5	47.1 ± 6.9	23.1 ± 8.4	76.9 ± 2.5	3.4 ± 0.5	20.0 ± 1.8	43.9 ± 4.6	27.2 ± 6.6
P samples										
Before	74.2 ± 5.6	4.7 ± 0.7	21.9 ± 2.8	49.8 ± 8.2	22.7 ± 11.9	72.1 ± 3.0	4.9 ± 0.7	23.1 ± 1.4	53.2 ± 4.2	17.4 ± 5.2
After	75.2 ± 6.6	4.5 ± 1.6	22.9 ± 3.0	51.1 ± 9.6	19.8 ± 10.9	77.0 ± 6.5	3.8 ± 1.5	21.3 ± 2.6	46.8 ± 8.5	24.3 ± 9.6
Bwh										
C samples										
Before	76.8 ± 5.7	3.3 ± 1.2	18.4 ± 2.7	41.2 ± 8.0	31.7 ± 10.6	76.1 ± 4.8	3.1 ± 1.0	21.5 ± 3.2	46.8 ± 7.8	20.9 ± 10.6
After	75.9 ± 6.0	3.6 ± 1.3	19.3 ± 3.0	43.5 ± 9.0	28.8 ± 11.1	76.8 ± 4.8	3.5 ± 1.2	19.2 ± 3.2	42.8 ± 8.7	29.5 ± 10.8
N samples										
Before	77.4 ± 2.8	3.6 ± 0.7	18.3 ± 2.3	40.9 ± 5.6	33.3 ± 7.6	74.0 ± 2.7	3.8 ± 0.6	23.6 ± 2.3	51.9 ± 5.4	14.6 ± 6.8
After	76.2 ± 2.7	3.9 ± 0.6	20.0 ± 2.0	44.6 ± 5.2	28.0 ± 7.0	75.3 ± 3.5	4.0 ± 0.9	20.9 ± 1.8	46.8 ± 5.4	24.4 ± 6.2
P samples										
Before	78.4 ± 5.0	3.6 ± 1.1	22.1 ± 5.1	47.1 ± 11.7	23.1 ± 16.8	76.9 ± 7.9	5.3 ± 1.4	23.4 ± 4.5	51.9 ± 12.7	22.8 ± 17.3
After	75.3 ± 8.8	4.4 ± 2.0	22.0 ± 4.5	49.6 ± 13.9	22.5 ± 16.4	76.3 ± 3.0	4.8 ± 0.4	23.2 ± 1.0	50.9 ± 3.5	21.2 ± 5.0

lime mixes (Arizzi et al., 2015a) were found here. The weathering tests, indeed, did not induce either the dark or the orange staining that occurred under the laboratory tests carried out in this previous study. Moreover, the ΔE^* values measured here ($1 < \Delta E^*_{C\ sample} < 7$; $1 < \Delta E^*_{N\ sample} < 4$; $2 < \Delta E^*_{P\ sample} < 8$) are much lower compared to those obtained in Arizzi et al. (2015a) ($\Delta E^*_{C\ sample} \sim 30$, $\Delta E^*_{N\ sample} \sim 13$, $\Delta E^*_{P\ sample} \sim 16$). This means that, under more realistic weathering conditions, hemp–lime mixes do not suffer visible colour modifications as may happen during laboratory water capillary rise and absorption tests. However, the standard tests were carried out for a longer period of time (4 weeks) compared to the weathering tests (12 days).

3.2. Microbial colonisation: identification and observation

The bacteria and fungi isolated in the hemp–lime samples are indicated in Table 3. In both control and tested samples, Gramme-positive bacilli (species of the genus *Bacillus*, forming either endospores or capsulated spores, Fig. 7a), Gramme-positive cocci (*Micrococcus* genus, and Staphylococcus, Fig. 7b) and other species of the Firmicutes and Actinobacteria phyla were detected. These bacteria are very common, as they are resistant to a wide range of temperature and relative humidity conditions. Also different types of filamentous fungi of the phylum Ascomycota and one basidiomycete yeast were isolated. Although no fungi were isolated in control samples, this does not guarantee their absence in samples, as only standard culture-based methods and not molecular DNA techniques have been used here (Ettenauer et al., 2012).

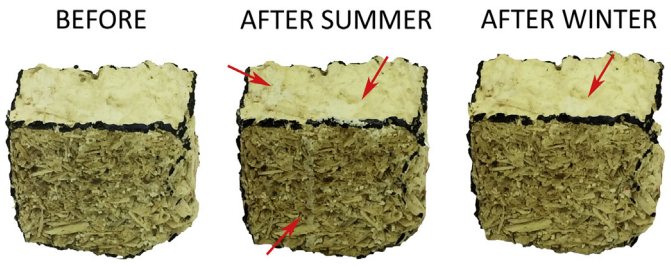

Fig. 6. Appearance of a P sample (CL90S PL + hemp shives mix) before, during and after Mediterranean (*Csa*) weathering test. Red arrows indicate the presence of white stains. (For interpretation of the references to colour in this figure legend, the reader is referred to the web version of this article.)

As expected due to the higher temperatures and relative humidity (Crispim et al., 2003) of the Af climate, microbial colonisation has been more intense under Tropical climatic conditions. In particular, a larger amount and diversity of microorganisms have formed in Af samples (ten different species of bacteria and six species of fungi were isolated). The isolated microorganisms may under represent those grown under Af simulations, as the washing effect of the rainfall simulated in the cabinet has certainly swept some spores away from the sample surface. It is worth noticing that Basidiomycetous yeast was isolated only in Af samples, as this type of microorganism needs more humidity than filamentous fungi to grow.

The Mediterranean climate has induced the growth of six species of bacteria and four species of fungi, with a moderate diversity, whilst in the arid climate only four species of bacteria and two species of fungi appeared.

All the isolated microorganisms are known to grow and survive both in the presence and absence of natural light.

Although climatic conditions are the main factor that affects bacterial and fungal colonisation (Shirakawa et al., 2010), in these tests there is no predominance of one type of microorganism over another depending on the climate. Most of the detected bacteria and fungi have a universal distribution and are often isolated under a wide range of environmental factors (such as temperature, pH and salinity) and nutrient concentration in the medium (Gaylarde and Gaylarde, 2005). Even under stressful environmental conditions, bacteria can

Table 3
Microorganisms isolated in the hemp–lime mix control and tested samples (treated and untreated with salt). Legend: C, CL90S + hemp shives mix; N, NHL 3.5 + hemp shives mix; P, CL90S PL + hemp shives mix; *Csa*, Mediterranean, *Af*, Tropical and *Bwh*, Semi-arid weathering tests.

Control samples

Treatment		Bacteria	Fungi
Without salt	*C*	Sporulated Gramme positive bacilli Gramme positive cocci (*Staphylococcus*)	–
	N	Gramme positive bacilli Gramme positive cocci (*Staphylococcus* and *Micrococcus*)	–
	P	Gramme positive cocci	–
With salt	*C*	Sporulated Gramme positive bacilli Capsulated Gramme positive bacilli Gramme positive cocci (*Staphylococcus* and *Micrococcus*)	–
	N	Capsulated Gramme positive bacilli Gramme positive cocci (*Staphylococcus* and *Micrococcus*)	–
	P	Capsulated Gramme positive bacilli Gramme positive cocci	–

Tested samples

Climate	Treatment		Bacteria	Fungi
Csa	*Without salt*	*C*	Sporulated Gramme positive bacilli Gramme positive bacilli (two different species) Gramme positive cocci (*Micrococcus*, *Sporosarcina*) Actinobacteria	*Aspergillus* *Penicillium rhizopus*
		N	Gramme positive bacilli (two different species) Gramme positive cocci (*Micrococcus*) Actinobacteria	*Acremonium* *Penicillium*
		P	Gramme positive bacilli *Arthrobacter* (Corinebacteria) Gramme positive bacilli	*Penicillium*
	With salt	*C*	Gramme positive bacilli (two different species) Sporulated Gramme positive bacilli Gramme positive cocci (*Micrococcus*) Gramme positive bacilli (Corinebacteria) Actinobacteria	*Aspergillus Penicillium* *Rhizopus*
		N	Sporulated Gramme positive bacilli Gramme positive bacilli (two different species) Gramme positive cocci (*Micrococcus*)	*Penicillium*, *Aspergillus*
		P	Sporulated Gramme positive bacilli Gramme positive cocci (*Micrococcus*)	*Penicillium*, *Aspergillus*
Af	*Without salt*	*C*	Sporulated Gramme positive bacilli Gramme positive bacilli (three different species) Gramme positive cocci (*Staphylococcus*)	*Acremonium* Basidiomycete yeast
		N	Sporulated Gramme positive bacilli Gramme positive cocci (*Micrococcus* and two different species)	*Penicillium* *Cladosporium* Unidentified fungus
		P	Capsulated Gramme positive bacilli (different specie)	
	With salt	*C*	Capsulated Gramme positive bacilli Gramme positive bacilli Gramme positive cocci (*Staphylococcus* and two different species)	*Penicillium*
		N	Sporulated Gramme positive bacilli Capsulated Gramme positive bacilli Gramme positive bacilli Capsulated Gramme positive cocci Gramme positive cocci	*Aspergillus* *Cladosporium* *Penicillium* Unidentified fungus
		P	Capsulated Gramme positive bacilli Gramme positive bacilli Gramme positive cocci (*Staphylococcus* and *Micrococcus*)	–
Bwh	*Without salt*	*C*	Gramme positive bacilli Gramme positive cocci (*Staphylococcus* and *Micrococcus*)	*Cladosporium*
		N	Capsulated Gramme positive bacilli Gramme positive cocci (*Staphylococcus* and *Micrococcus*)	–
		P	Gramme positive cocci(irregular mucilaginous masses)	–
	With salt	*C*	Capsulated Gramme positive bacilli Gramme positive cocci (*Staphylococcus* and *Micrococcus*)	*Cladosporium* *Penicillium*
		N	Gramme positive bacilli Capsulated Gramme positive cocci Gramme positive cocci (*Micrococcus*)	*Penicillium*
		P	Capsulated Gramme positive bacilli Gramme positive cocci (*Staphylococcus* and *Micrococcus*)	–

produce endospores. Members of the phylum Firmicutes (included *Sporosarcina*, *Bacillus* and *Paenibacillus* species) are alkaliphiles and halophiles, psychrophiles or psychrotrophs and some of them are thermophiles. The genera *Micrococcus* and *Arthrobacter*, belonging to the phylum actinobacteria, are equally adapted to environmental factors for their structural characteristics. Therefore, both are able to grow in many different environments. Most of the identified fungi belong to the Ascomycota division, being the genera *Penicillium* (Fig. 7c) and *Aspergillus* (Fig. 7d) the most frequent. They have great capacity to tolerate fluctuating environmental conditions and withstand environmental stress (Pasanen et al., 2000a,b). However, the frequent fluctuations of T and RH simulated here may have hindered further colonisation of fungi in samples. The isolated fungi are likely to colonise and grow on the surface (or few millimetres from the surface) of the hemp–lime materials, as long as the external conditions are humid enough for the fungi to survive. In the opposite case (scarce moisture content), fungi can

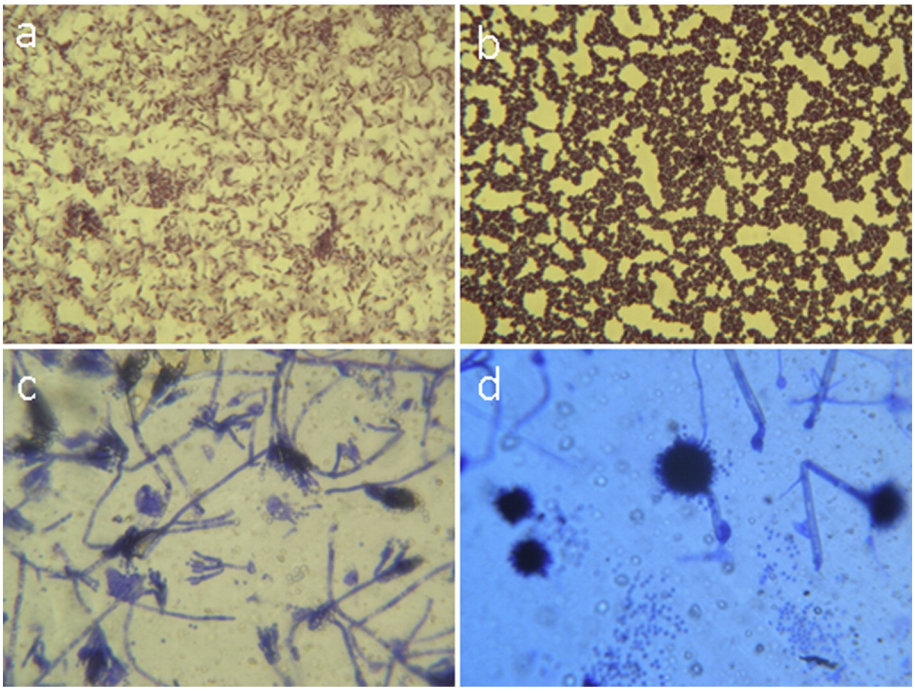

Fig. 7. Microscopic images of bacteria (a and b) and fungi (c and d) isolated from the hemp–lime samples under the Mediterranean (*Csa*) weathering test: (a) Gramme-positive bacilli (1250×); (b) Gramme-positive cocci (1250×); (c) *Penicillium* (787×); (d) *Aspergillus* (787×).

penetrate inside the material by developing hyphae, more or less deep depending on the porosity and permeability of the matrix towards oxygen. For this reason, fungi are more likely to survive in arid environments compared to other microorganisms, such as bacteria (Staley et al., 1982; Cutler and Viles, 2010).

The microbial activity on the samples was also recognised during ESEM observations that showed the presence of a biofilm (probably EPS, extracellular polymeric substance), in the form of a dark layer that covered the matrix (Fig. 8a). This layer tended to break and volatilize (Fig. 8b and c) under the continuous incidence of electrons in the chamber (for example, during focusing), which confirms its organic nature. Most of the isolated bacteria are capsulated (cocci and bacilli), which facilitates the adhesion to the substrate and, therefore, the creation of a biofilm. The presence of biofilm on the hemp–lime mixes represents a cause of decay because, although it reduces the water capillary uptake due to a closing of pores, it also decreases the water vapour permeability of the material, reducing evaporation (Cutler and Viles, 2010).

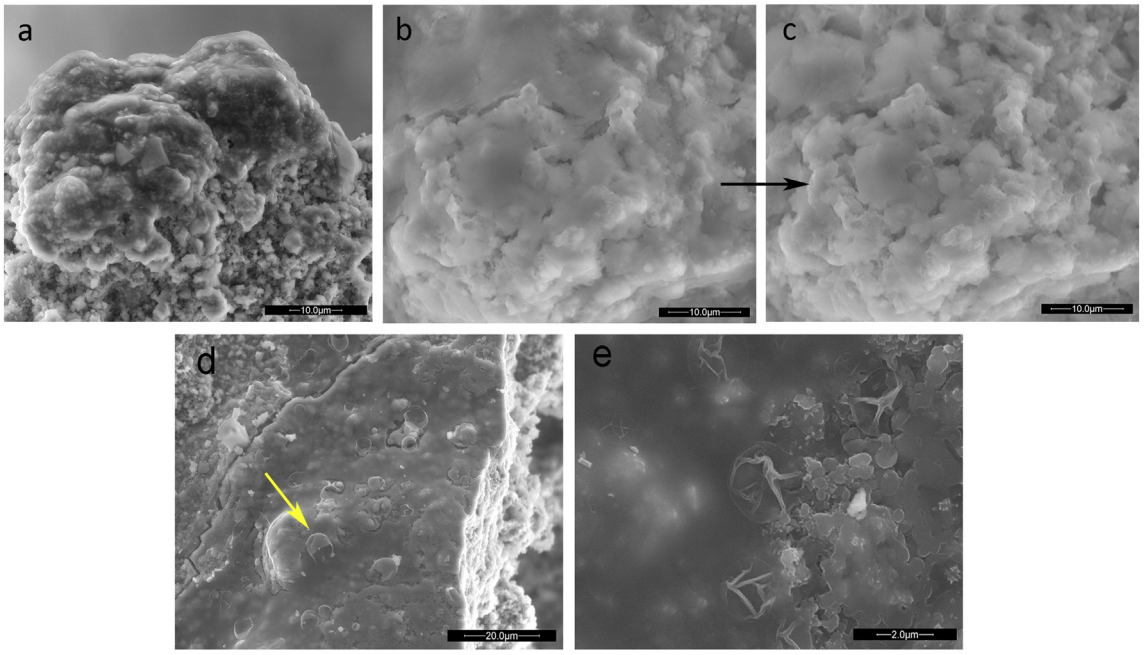

Fig. 8. ESEM images of C (CL90S + hemp shives mix; a, b and c) and P (CL90S PL + hemp shives mix; d and e) samples subjected to the Mediterranean (*Csa*) weathering test. The black arrow in b and c indicates how the biofilm broke during focusing. The yellow arrow in d indicates empty spores of fungi. (For interpretation of the references to colour in this figure legend, the reader is referred to the web version of this article.)

Moreover, many empty and thin-walled round particles similar to spores were observed embedded in the EPS (2–10 μm in diameter, indicated by the arrow in Fig. 8d and e). Some of them maintained the same shape after relative humidity changes in the ESEM chamber (Fig. 8d), others instead appeared permanently dehydrated (Fig. 8e). Spores of fungi were also observed in a previous weathering study performed on the same hemp–lime mixes (Arizzi et al., 2014).

The absence of hyphae in the hemp–lime samples might be due to the fact that fungi do not need to penetrate deeper in the matrix, as both nutrients (polysaccharides from the hemp) and moisture (relative humidity of the environment) are available at the surface. It is also possible that superficial washing during rainfall periods had caused a lack of hyphae, especially if acting in the initial phase of their formation.

3.3. Sample's mineralogy and morphology

After three months of hardening, the control samples still present large amounts of the binder phases, such as portlandite (between 6 and 30%, Table 4) and calcium silicates (15–20%, Table 4). Moreover, part of the carbonated portlandite has transformed into vaterite (up to 30%, Table 4).

Table 4
Mineral phases (amount in %) of hemp–lime mix control and tested samples (treated and untreated with salt). Legend: C, CL90S + hemp shives mix; N, NHL 3.5 + hemp shives mix; P, CL90S PL + hemp shives mix; *Csa*, Mediterranean, *Af*, Tropical and *Bwh*, Semi-arid weathering tests; Cal, calcite ($CaCO_3$); Por, portlandite ($CaOH_2$); Vat, vaterite ($CaCO_3$); CS, calcium silicates ($CaSiO_3$/Ca_2SiO_4); Hal, halite (NaCl); —, absent; *, 2–5%; **, 6–10%; ***, 11–20%; ****, 21–40%; *****, 41–50%; ******, 51–60%; *******, 61–85%. Calcite and vaterite are polymorphs of the same chemical compound.

	Cal	Por	Vat	CS	Hal
Control samples					
C					
Without salt	*******	****	**	–	–
With salt	******	***	**	–	***
N					
Without salt	******	**	****	***	–
With salt	*****	**	***	***	**
P					
Without salt	*****	****	****	–	–
With salt	*****	****	***	–	***
Csa samples					
C					
Without salt	*****	****	***	–	–
With salt	*****	****	****	–	*
N					
Without salt	*****	**	****	****	–
With salt	*****	*	****	***	*
P					
Without salt	****	*****	****	–	–
With salt	*****	****	***	–	**
Af samples					
C					
Without salt	*******	**	***	–	–
With salt	*******	*	**	–	*
N					
Without salt	******	*	****	***	–
With salt	******	*	***	**	*
P					
Without salt	******	*	*****	–	–
With salt	******	*	****	–	*
Bwh samples					
C					
Without salt	******	****	**	–	–
With salt	*******	**	***	–	**
N					
Without salt	*******	**	***	***	–
With salt	******	*	***	***	**
P					
Without salt	*******	***	***	–	–
With salt	*******	*	*	–	***

The identification of vaterite in hemp–lime mixes has been recently discussed and inferred to result from a scarce amount of water in the matrix, which delays the transformation of vaterite into calcite from the beginning (Arizzi et al., 2015b). If this interpretation is correct, we should expect more calcite to be formed under the humid conditions of the Af climate, due to both portlandite and vaterite transformation. Vice versa, under the arid conditions of the Bwh climate, more vaterite should be formed from the carbonation of portlandite. Notwithstanding, XRD results show that higher amounts of vaterite were present in samples subjected to the Mediterranean and Tropical weathering conditions, compared to the Semi-arid ones (Table 4). This suggests that the insufficient moisture in the matrix of hemp–lime mixes cannot be the only cause of precipitation and stabilisation of vaterite.

Owing to the presence in the hemp–lime mixes of *bacilli* (Table 3) that might potentially precipitate carbonates and of fungi, which have the ability to transform and precipitate secondary minerals (as they excrete acids, protons and other metabolites, Fomina et al., 2010), and due to the presence of organic substances released both by these microorganisms and the hemp itself (Diquélou et al., 2015), we may interpret the formation of calcium carbonate as a bacterially-mediated process (instead of insufficient water). In high pH environments, indeed, the bacterial cells have a negative charge on their surface and this indicates that they can act as nucleation sites for carbonate to precipitate (Williams et al., 2015). Several studies on the bacterially-mediated precipitation of carbonates have shown that the bacterial activity and the presence of organic molecules (bacterium cell walls, EPS and organic by-products of bacterial activity) indeed promote especially the formation and stabilisation of vaterite, which precipitates in the form of spherulites that sometimes encapsulate bacterial cells (Rodriguez-Navarro et al., 2007; Sanchez-Navas et al., 2009; Rodriguez-Navarro et al., 2012). The microbiological, mineralogical and morphological studies on the hemp–lime mixes support this assumption. XRD results show that, together with the growth of more types of microorganisms (Table 3), more vaterite is formed under the Mediterranean and Tropical climate compared to the Semi-Arid one (Table 4). Furthermore, ESEM observations of the hemp–lime mixes (especially those made with aerial lime, C and P) show that many rounded framboids (the majority of them with diameters of 2–5 μm, Fig. 9) are formed. All of them are reminiscent of the shape of vaterite spherulites (Andreassen, 2005; Nehrke and Van Cappellen, 2006; Schmidt et al., 2010; Rodriguez-Navarro et al., 2007; Rodriguez-Navarro et al., 2012), even though the nanometric crystals grown on their surface have the scalenohedral habit of calcite. This indicates that a transformation of vaterite into calcite has occurred on the surface of the framboidal particles during simulations in the environmental cabinet, as observed elsewhere (Nehrke and Van Cappellen, 2006; Rodriguez-Navarro et al., 2007; Schmidt et al., 2010).

Moreover, oval shell-like formations of 25–40 μm in size (Fig. 9a), composed of a thin layer (of approximately 2 μm, indicated by the yellow arrows in Fig. 9b) of scalenohedral crystals of calcite (Fig. 9c) were observed. Although these shell-like formations are much bigger in size than the surrounding spheroidal particles of carbonates (Fig. 9d), their bacterial origin cannot be discarded, as a previous study has shown the bacterial formation of carbonate spherulites with sizes up to hundreds micrometres (Sanchez-Navas et al., 2009).

3.4. Salt crystallisation

The mineralogical analysis on the control samples treated with salt confirms that mixes made with aerial lime (C and P samples) absorbed more salt compared to the natural hydraulic lime ones, especially those made with lime putty (up to 20% of halite identified, Table 4). As also demonstrated by the weight loss of samples during the test (Fig. 3), the washing action of water during heavy and frequent rainfall simulated under the Af test caused very little precipitation of halite crystals (only 2–5% of halite identified by XRD, Table 3). On the contrary, due

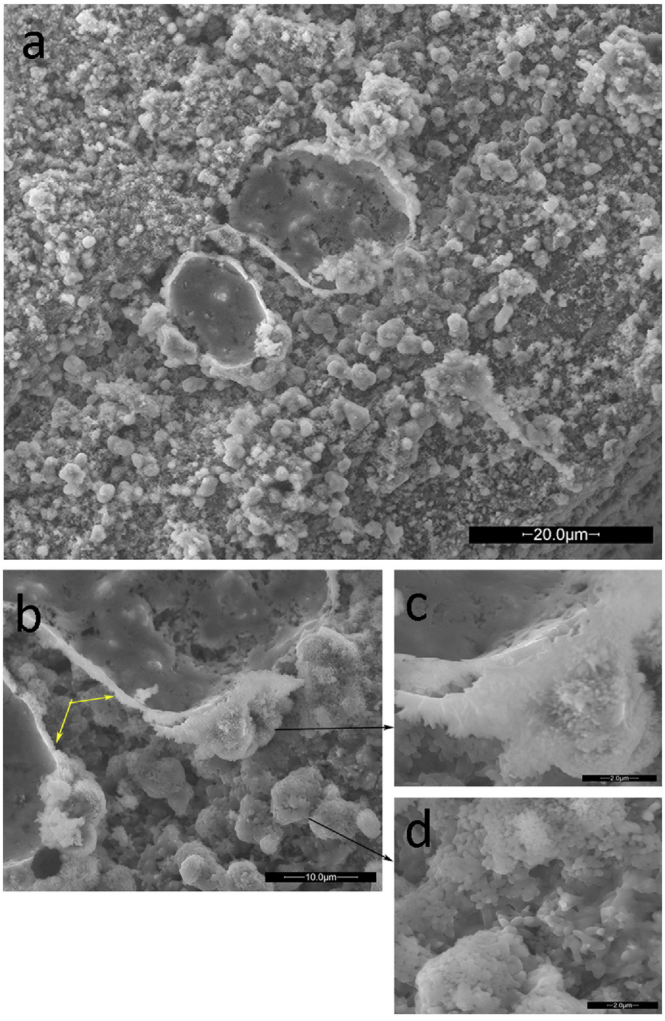

Fig. 9. ESEM images of a P sample (CL90S PL + hemp shives mix) subjected to the Mediterranean (*Csa*) weathering test: (a, scale bar: 20 µm, and b, scale bar: 10 µm) oval shell-like formations and small framboids (20 µm); (c, scale bar: 2 µm) detail of the external layer; (d, scale bar: 2 µm) surrounding matrix. The yellow arrows in b indicate the thin layer of calcite crystals. The black arrows indicate the areas in b that can be observed at higher magnification in c and d. (For interpretation of the references to colour in this figure legend, the reader is referred to the web version of this article.)

to the lower amount of water sprayed during rainfall simulation under Semi-arid climatic conditions, a higher salt content, similar to that in control samples treated with salt, was found in the Bwh samples (Fig. 10).

Morphologies typical of halite (cubic, irregular shaped and rods, Lubelli et al., 2010) were observed in the samples subjected to Bwh simulations (Fig. 10) and, similarly, in Csa samples. Contrary to other soluble salts, such as sodium or magnesium sulphates that cause a deeper damage as they crystallise inside porous materials (Benavente et al., 2004), sodium chloride forms a superficial layer on the sample matrix, in a similar way as described in Walker et al.'s (2014) study, although the salt layers observed here are less extended and smooth, owing to different salt concentration and application time and conditions. When comparing control (not weathered) and weathered samples pre-treated with salt the only difference is the amount of salt, which is bigger in the former, whilst salt morphologies are the same in both types of samples.

Although ESEM observations were carried out at a relative humidity (RH ~ 55%) below the halite critical RH (76%), so as to ensure the salt stability inside the chamber, a wider range of relative humidity values was established during purging (50 < RH < 100%) in order to achieve the equilibrium prior to observation. These prior conditions might have caused dissolution and re-precipitation of the halite crystals in other areas of the observed samples, as well as a change in the morphology of the crystals. Relative humidity cycles performed to induce dissolution and re-precipitation of the salt inside the ESEM chamber demonstrate this assumption (see Supplementary material SM 3).

4. Conclusions

The weathering conditions simulated in this study (Mediterranean, Tropical and Semi-arid climatic conditions) do not cause significant macroscopic changes in hemp–lime renders. Mass, volume and appearance of the material remain almost unvaried, with only slight noticeable differences after heavy rainfall (mass uptake) and in samples made with aerial lime (yellowing of the surface). Under the simulated climatic conditions the hardening process of both aerial and natural hydraulic lime mixes is improved compared to control mixes (especially under Tropical climate), because further carbonation of portlandite and, in some cases, bacterially-mediated precipitation of calcium carbonates (especially under Mediterranean climate) are promoted.

The colonisation and growth of different alkaliphiles (or alkalitolerant) fungi (such as *Acremonium*, *Penicillium* and *Aspergillus*) and bacteria (such as *Bacillus*, *Arthrobacter* and *Micrococcus*) under the three climatic conditions have demonstrated that the bio-receptivity of hemp–lime cannot be disregarded when predicting its long-term durability (*c.f.* other mortars not used in these experiments). Although no climate-related predominance has been observed among the isolated microorganisms, the water intake (as relative humidity and rainfall) seems to be critical for the existence of a greater diversity of species in samples, as it occurs under the Tropical climate. None of the isolated microorganisms have caused either aesthetic changes or physical breakdown during or after the test and this encourages the use of hemp–lime renders under Mediterranean, Semi-arid and Tropical climates. However, under realistic climatic conditions the microbial activity may be enhanced in hemp-based materials, with negative consequences for the long-term vulnerability of a material to chemical and physical weathering, unless it is not intended as bio-protector. Biocide

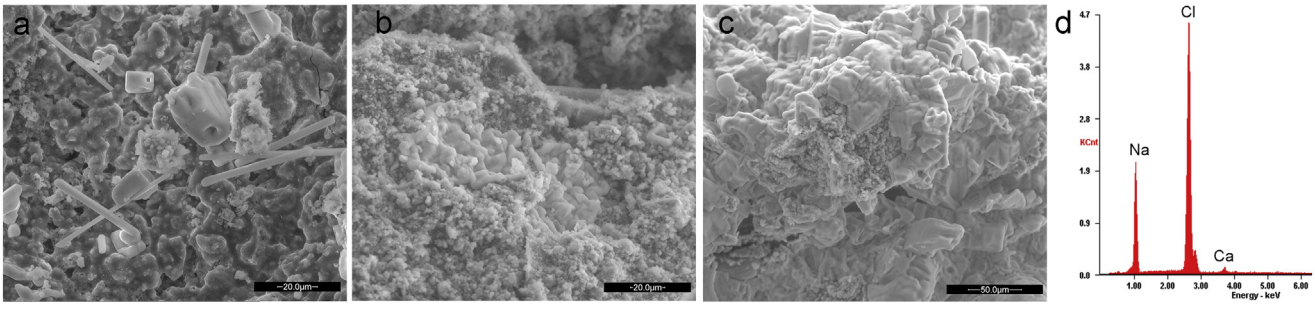

Fig. 10. ESEM images (a, b and c) and EDX spectrum (d) of NaCl deposition in hemp–lime samples treated with salt and subjected to the Semi-arid (*Bwh*) weathering test. Legend: C, CL90S + hemp shives mix (scale bar: 20 µm); N, NHL 3.5 + hemp shives mix (scale bar: 20 µm); P, CL90S PL + hemp shives mix (scale bar: 50 µm).

treatments such as gamma irradiation of the hemp or addition of anti-microbial (non-acrylic) products or nanoparticles in the formulation to increase the material resilience towards the attack of bacteria and fungi could be possible solutions that are worth of further investigations.

Salt weathering due to sodium chloride does not induce breakdown in the hemp–lime renders under any of the climatic conditions reproduced here. The main reason is that NaCl precipitates superficially and is easily removed by leaching from the material especially when rainfall is heavy and frequent (like in Tropical areas). Under low rainfall, typical of the Semi-arid climate, more salt is absorbed but still no damage can be observed in the material. A more intense salt weathering of the hemp–lime mixes could be expected in foggy coastal desert areas, due to the frequent wetting-drying cycles associated to the fog events that induce numerous cycles of sodium chloride dissolution-crystallisation (Goudie and Parker, 1998). However, the hygroscopic nature of hemp ensures moisture being retained longer in the material, with the result that salt weathering due to natural wetting-drying cycles can be less aggressive than in other inorganic porous materials (such as stone and mortar).

It should be pointed out that although the experimental setup designed here to study the durability of hemp–lime mixes under different climatic conditions is not sufficient to assess meaningful changes in the integrity of these materials, our experiments have shown a different behaviour of the mixes according to the lime used and the climatic conditions applied. This is certainly a significant basis on which it will be possible to set up future studies. Future investigations on the durability of the same materials exposed to outdoor environmental conditions would help overcome the limitations of the current study.

As a final remark, we emphasise the potential of this work to become a reference for future laboratory studies on the durability of building materials, as long as they lie in the proposed methodology: 1) designing and performing more realistic weathering simulations according to the climatic conditions of the area of interest; 2) following macroscopic (mass, volume, colour, appearance) and microscopic (morphology and mineralogy of phases, microbial growth) changes in samples during and after the test; 3) interpreting the material behaviour as a combination of extrinsic (environmental conditions) and intrinsic (chemical, mineralogical and textural properties, e.g. pore system, of the material) factors.

Acknowledgements

This study was financially supported by the European Commission under the Marie Curie programme (FP7-PEOPLE-2012-IEF call, research project “NaturaLime”) and by the Spanish research project MAT-2012-34473. We are grateful to Arch. Monika Brummer (Cannabric company, Spain, www.cannabric.com) for providing the hemp and preparing the mixes, as well as for her suggestions about the choice of the simulated climates.

Appendix A. Supplementary data

Supplementary data to this article can be found online at http://dx.doi.org/10.1016/j.scitotenv.2015.10.141.

References

Aït Oumeziane Y, Bart M, Moissette S, Lanos C, Collet F, Pretot S. Hysteresis phenomenon in hemp concrete. Proceedings of the 1st International Conference on Bio-Based Building Materials. Eds.: Amziane S & Sonebi M, Associate Ed.: Charlet K; RILEM Publications S.A.R.L.; ISBN PRO 99: 978-2-35158-154-4; 2015.

Altieri A, Pinna D. Monumenti e manufatti in ambienti costieri. La biologia vegetale per i Beni Culturali. Vol. I Biodeterioramento e conservazione. Caneva G. Nugari M.P., Salvadori O. Collana Arte e Restauro, Nardini Ed., Firenze; 2005: 196-9.

Andreassen, J.P., 2005. Formation mechanism and morphology in precipitation of vaterite-nano-aggregation or crystal growth? J. Cryst. Growth 274, 256–264.

Arizzi, A., Viles, H., Martin-Sanchez, I., Cultrone, G., 2014. Testing the durability of hemp-based mortars under Mediterranean climatic conditions in coastal and inland areas: does the presence of salt alter hemp bioreceptivity? SWBSS2014, 3rd International Conference on Salt Weathering of Buildings and Stone Sculptures, Bruxelles

Arizzi, A., Brümmer, M., Martín-Sanchez, I., Cultrone, G., Viles, H., 2015a. The influence of the type of lime on the hydric behaviour and bio-receptivity of hemp lime composites used for rendering applications in sustainable new construction and repair works. PloS One 1–19 http://dx.doi.org/10.1371/journal.pone.0125520.

Arizzi, A., Cultrone, G., Brümmer, M., Viles, H., 2015b. A chemical, morphological and mineralogical study on the interaction between hemp hurds and aerial and hydraulic lime particles: implications for mortar manufacturing. Constr. Build. Mater. 75, 375–384.

ASTM E313-15, 2015. Standard Practice for Calculating Yellowness and Whiteness Indices from Instrumentally Measured Color Coordinates. ASTM International, West Conshohocken, PA.

Benavente, D., García del Cura, M.A., García-Guinea, J., Sánchez-Moral, S., Ordónez, S., 2004. Role of pore structure in salt crystallisation in unsaturated porous stone. J. Cryst. Growth 260, 532–544.

Bessette L, Tremerie B, Bejat T, Piot A, Jay A, Barnes Davin L. Study of the development of mould on prompt natural cement-based hemp concrete. Proceedings of the 1st International Conference on Bio-Based Building Materials. Eds.: Amziane S & Sonebi M, Associate Ed.: Charlet K; RILEM Publications S.A.R.L.; ISBN PRO 99: 978-2-35158-154-4; 2015.

Bevan R, Woolley T. Hemp Lime Construction. A Guide to Building With Hemp Lime Composites. HIS BRE Press, Bracknell, UK; 2008:41-2. ISBN: 978-1-84806-033-3.

BS-EN 15886, 2010. Conservation of Cultural Property. Test Methods. Colour Measurement of Surfaces. BSI, Standards Publication, London.

BS-EN 459-1, 2010. Building Lime. Part 1: Definitions, Specifications and Conformity Criteria. BSI, Standards Publication, London.

Camuffo D. Microclimate for Cultural Heritage. Conservation, Restoration and Maintenance of Indoor and Outdoor Monuments. Second Edition, Elsevier, USA; 2014:6. ISBN: 978-0-444-63296-8.

Caneva, G., Gori, E., Danin, A., 1992. Incident rainfall in Rome and its relation to biodeterioration of buildings. Atmos. Environ. 26B (2), 255–259.

Crispim, C.A., Gaylarde, P.M., Gaylarde, C.C., 2003. Algal and cyanobacterial biofilms on calcareous historic buildings. Curr. Microbiol. 46, 79–82.

Cutler, N., Viles, H., 2010. Eukaryotic microorganisms and stone biodeterioration. Geomicrobiol J. 27, 630–646.

Diquélou, Y., Gourlay, E., Arnaud, L., Kurek, B., 2015. Impact of hemp shiv on cement setting and hardening: influence of the extracted components from the aggregates and study of the interfaces with the inorganic matrix. Cem. Concr. Compos. 55, 112–121.

Esmail, A., 2010. Cannabis Sativa: an optimization study for ROI. Bachelor of Science in Mechanical Engineering, Massachusetts Institute of Technology.

Ettenauer, J.D., Pinar, G., Lopandic, K., Spangl, B., Ellersdorfer, G., Voitl, C., Sterflinger, K., 2012. Microbes on building materials — evaluation of DNA extraction protocols as common basis for molecular analysis. Sci. Total Environ. 439, 44–53.

Faruk, O., Bledzki, A.K., Fink, H.P., Sain, M., 2012. Biocomposites reinforced with natural fibers: 2000-2010. Prog. Polym. Sci. 37, 1552–1596.

Fomina, M., Burford, E.P., Hillier, S., Kierans, M., Gadd, G.M., 2010. Rock-building fungi. Geomicrobiol J. 27, 624–629.

Gaylarde, C.C., Gaylarde, P.M., 2005. A comparative study of the major microbial biomass of biofilms on exteriors of buildings in Europe and Latin America. Int. Biodeterior. Biodegrad. 55, 131–139.

Goudie, A.S., Parker, A.G., 1998. Experimental simulation of rapid rock block disintegration by sodium chloride in a foggy coastal desert. J. Arid Environ. 40, 347–355.

Jain, A., Bhadauria, S., Kumar, V., Singh, C.R., 2009. Biodeterioration of sandstone under the influence of different humidity levels in laboratory conditions. Build. Environ. 44, 1276–1284.

Johansson, P., Ekstrand-Tobin, A., Bok, G., 2014. An innovative test method for evaluating the critical moisture level for mould growth on building materials. Build. Environ. 81, 404–409.

Kottec, M., Grieser, J., Beck, C., Rudolf, B., Rubel, F., 2006. World map of the Köppen–Geiger climate classification updated. Meteorol. Z. 15 (3), 259–263.

Lamoulie J, Le Bayon I, Draghi M, Roger M, Pompeo C, Gabille M, Pregnac M, Jequel M, Kutnik M. Use of bio-based insulation materials in buildings: modelling of the hygrothermal conditions in use — resistance of a wood fibre material to moulds according to climatic conditions. Proceedings of the 1st International Conference on Bio-Based Building Materials. Eds.: Amziane S & Sonebi M, Associate Ed.: Charlet K; RILEM Publications S.A.R.L.; ISBN PRO 99: 978-2-35158-154-4; 2015.

Lubelli, B., Nijland, T.G., van Hees, R.P.J., Hacquebord, A., 2010. Effect of mixed crystallization inhibitor on resistance of lime–cement mortar against NaCl crystallization. Constr. Build. Mater. 24, 2466–2472.

Manso, S., De Muynck, W., Segura, I., Aguado, A., Steppe, K., Boon, N., De Belie, N., 2014. Bioreceptivity evaluation of cementitious materials designed to stimulate biological growth. Sci. Total Environ. 481, 232–241.

Marceau S, Gle P, Gueguen E, Gourlay E, Moscardelli S, Nour I, Amziane S, Abdellaoui L. Assessment of the durability of bio-based insulating materials. Proceedings of the 1st International Conference on Bio-Based Building Materials. Eds.: Amziane S & Sonebi M, Associate Ed.: Charlet K; RILEM Publications S.A.R.L.; ISBN PRO 99: 978-2-35158-154-4; 2015.

Martín Ramos, J.D., 2004. XPowder. A Software Package for Powder X-ray Diffraction Analysis. Lgl. Dep. GR 1001/04.

Nehrke, G., Van Cappellen, P., 2006. Framboidal vaterite aggregates and their transformation into calcite: a morphological study. J. Cryst. Growth 87, 528–530.

Pasanen, A.L., Kasanen, J.P., Rautiala, S., Ikäheimo, M., Rantamäki, J., Kääriäinen, H., Kalliokoski, P., 2000a. Fungal growth and survival in building materials under fluctuating moisture and temperature conditions. Int. Biodeterior. Biodegrad. 46 (2), 117–127.

Pasanen, A.L., Rautiala, S., Kasanen, J.P., Raunio, P., Rantamaki, J., Kalliokoski, P., 2000b. The relationship between measured moisture conditions and fungal concentrations in water-damaged building materials. Indoor Air 10 (2), 111–120.

Pervaiz, M., Sain, M.M., 2003. Carbon storage potential in natural fiber composites. Resour. Conserv. Recycl. 39, 325–340.

Rodriguez-Navarro, C., Jimenez-Lopez, C., Rodriguez-Navarro, A., Gonzalez-Munoz, M.T., Rodriguez-Gallego, M., 2007. Bacterially mediated mineralization of vaterite. Geochim. Cosmochim. Acta 71, 1197–1213.

Rodriguez-Navarro, C., Jroundi, F., Schiro, M., Ruiz-Agudo, E., González-Muñoz, M.T., 2012. Influence of substrate mineralogy on bacterial mineralization of calcium carbonate: implications for stone conservation. Appl. Environ. Microbiol. 78 (11), 4017–4029.

Sanchez-Navas, A., Martin-Algarra, A., Rivadeneyra, M.A., Melchor, S., Martin-Ramos, J.D., 2009. Crystal-growth behaviour in Ca–Mg carbonate bacterial spherulites. Cryst. Growth Des. 9 (6), 2690–2699.

Schmidt, M., Stumpf, T., Walther, C., Geckeis, H., Fanghänel, T., 2010. Phase transformation in $CaCO_3$ polymorphs: a spectroscopic, microscopic and diffraction study. J. Colloid Interface Sci. 351, 50–56.

Shirakawa, M.A., Goncalves Tavares, R., Gaylarde, C.C., Santos Taqueda, M.E., Loh, K., Vanderley, M.J., 2010. Climate as the most important factor determining anti-fungal biocide performance in paint films. Sci. Total Environ. 408, 5878–5886.

Simons A, Bertron A, Aubert JE, Laborel-Preneron A, Roux C, Roques C. Development of microorganism sampling methods on bio-based earth products for healthy, sustainable buildings. Proceedings of the 1st International Conference on Bio-Based Building Materials. Eds.: Amziane S & Sonebi M, Associate Ed.: Charlet K; RILEM Publications S.A.R.L.; ISBN PRO 99: 978-2-35158-154-4; 2015.

Staley, J.T., Palmer, F., Adams, J.B., 1982. Microcolonial fungi: common inhabitants on desert rocks? Science 215 (4536), 1093–1095.

Tran Le, A.D., Maalouf, C., Mai, T.H., Wurtz, E., Collet, F., 2010. Transient hygrothermal behaviour of a hemp concrete building envelope. Energy and Build 42, 1797–1806.

Walker, R., Pavia, S., Mitchell, R., 2014. Mechanical properties and durability of hemp–lime concretes. Constr. Build. Mater. 61, 340–348.

Williams SL, Kirisits MJ, Ferron RD. Characterization of live, dead, starved and heat-treated *S. pasteuri* cells: implications for biomineralization in construction materials. Proceedings of the 1st International Conference on Bio-Based Building Materials. Eds.: Amziane S & Sonebi M, Associate Ed.: Charlet K; RILEM Publications S.A.R.L.; ISBN PRO 99: 978-2-35158-154-4; 2015.